

# Chiral Hybrid Inorganic–Organic Materials: Synthesis, Characterization, and Application in Stereoselective Organocatalytic Cycloadditions

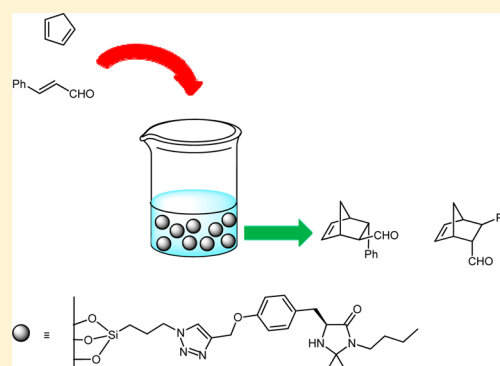
Alessandra Puglisi,\* Maurizio Benaglia, Rita Annunziata, Valerio Chiroli, Riccardo Porta, and Antonella Gervasini

Dipartimento di Chimica, Università degli Studi di Milano, Via Golgi 19, 20133, Milano, Italy

## Supporting Information

**ABSTRACT:** The synthesis of chiral imidazolidinones on mesoporous silica nanoparticles, exploiting two different anchoring sites and two different linkers, is reported. Catalysts 1–4 were prepared starting from L-phenylalanine or L-tyrosine methyl esters and supporting the imidazolidinone onto silica by grafting protocols or azide–alkyne copper(I)-catalyzed cycloaddition. The four catalysts were fully characterized by solid-state NMR, N<sub>2</sub> physisorption, SEM, and TGA in order to provide structural assessments, including an evaluation of surface areas, pore dimensions, and catalyst loading. They were used in organocatalyzed Diels–Alder cycloadditions between cyclopentadiene and different aldehydes, affording results comparable to those obtained with the nonsupported catalyst (up to 91% yield and 92% ee in the model reaction between cyclopentadiene and cinnamic aldehyde). The catalysts were recovered from the reaction mixture by simple filtration or centrifugation.

The most active catalyst was recycled two times with some loss of catalytic efficiency and a small erosion of ee.



## INTRODUCTION

With the advent of combinatorial chemistry many solid-phase methodologies have been developed where the substrates are immobilized on a solid support while the reagents are passed through in the mobile phase.<sup>1</sup> While after 20 years of intense activity in the field it is still a matter of discussion whether medicinal chemistry and the pharmaceutical industry have really taken advantage of combinatorial methods,<sup>2</sup> it is evident that organic synthesis has somehow been revolutionized since the importance and the opportunities offered by automation and advanced technologies became clear to synthetic chemists.<sup>3</sup> For example, the need for more and more efficient high-speed parallel synthesis, largely employed by pharmaceutical companies for lead discovery and optimization, led to the development of alternative solution-phase techniques utilizing supported reagents or scavengers.<sup>4</sup> Solid-phase-assisted synthesis is only one of the so-called *enabling technologies*, developed with the aim of speeding up the synthetic transformation and facilitating the isolation and purification of the final product.<sup>5</sup>

While immobilized reagents and scavengers have found widespread application in organic synthesis, the use of supported catalysts, and especially of chiral catalytic species, is much less common. Heterogenization can potentially provide easily recyclable and reusable solid catalysts<sup>6</sup> that have evenly distributed and precisely engineered active sites, similar to those of their homogeneous counterparts, and therefore could combine the advantages of both homogeneous and heterogeneous systems. Many immobilization approaches have been explored,

including the attachment of the chiral catalysts to organic polymers, dendrimers, membrane supports, and porous inorganic oxides and via biphasic systems.<sup>7</sup> Along this line, the immobilization of a chiral organic catalyst seems particularly attractive, because the metal-free nature of these compounds avoids from the outset the problem of the leaching of the metal, which often negatively affects and practically prevents the efficient recycling of a supported organometallic catalyst.<sup>8</sup> One of the most popular and versatile classes of chiral metal-free catalysts is that of chiral imidazolidinones,<sup>9</sup> the so-called MacMillan catalysts. These compounds have been covalently immobilized on both soluble<sup>10</sup> and insoluble supports.<sup>11</sup> In 2006 a properly modified enantiopure first-generation MacMillan imidazolidinone was anchored to novel siliceous mesocellular foams,<sup>12</sup> and more recently it has been immobilized in the pores of silica gel with the aid of an ionic liquid,<sup>13</sup> on hollow periodic mesoporous organosilica spheres<sup>14a</sup> and on magnetic nanoparticles.<sup>14b</sup> Despite this variety of proposed solutions, however, the development of an easily available, inexpensive, and truly efficient recoverable MacMillan catalyst has yet to be realized. Lower enantioselectivities with respect to that of the nonsupported system and recyclability are issues still waiting for a satisfactory solution. Because of the high surface area and the well-ordered structure, mesoporous silica may be considered as an ideal support for the preparation of

Received: August 24, 2013

Published: October 17, 2013

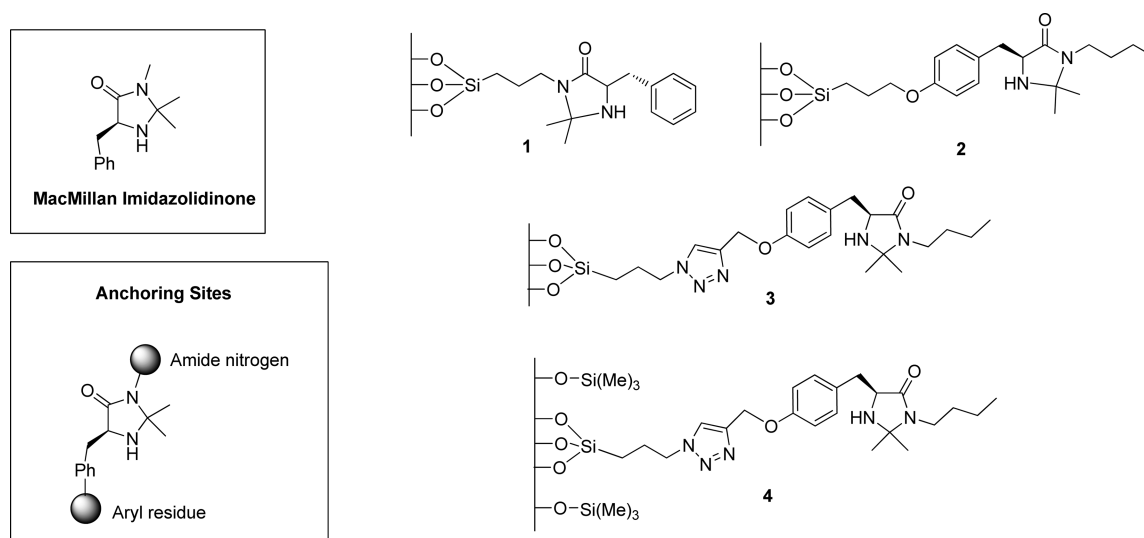
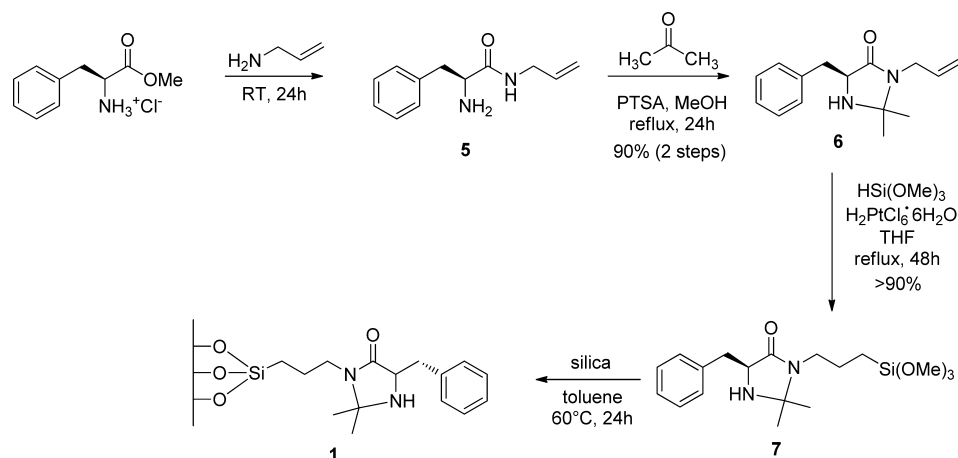


Figure 1. MacMillan imidazolidinone and silica-supported imidazolidinones.

### Scheme 1. Synthesis of Supported Imidazolidinone 1



heterogeneous catalysts and may help to positively address those problems.<sup>15</sup>

Basically two synthetic protocols are available to obtain mesoporous silica-supported catalysts: the cocondensation method and postsynthetic grafting. In addition, the nature of the cocondensation process, which involves the reaction of a tetralkoxysilane with organotrialkoxysilanes carrying the different functionalities required for catalysis, can open access to systems in which the functional group ratios can be varied at will, allowing an additional tuning of the catalyst's properties. A few years ago we developed a bifunctional catalytic system supported on mesoporous silica featuring tertiary amine and thiourea functionalities in different ratios, where the cooperativity of the two catalytically active sites was demonstrated in the conjugate addition of acetylacetone to 2-nitrostyrene.<sup>16</sup> On the basis of our previous experience we decided to investigate the use of these materials as supports also for chiral organic catalysts. In this work we report the preparation of a silica-supported MacMillan catalyst through different immobilization strategies, the characterization of the functionalized materials, and the study of their catalytic behavior in stereoselective Diels–Alder reactions; finally, the recovery and the recyclability of the supported chiral organocatalysts were also studied.

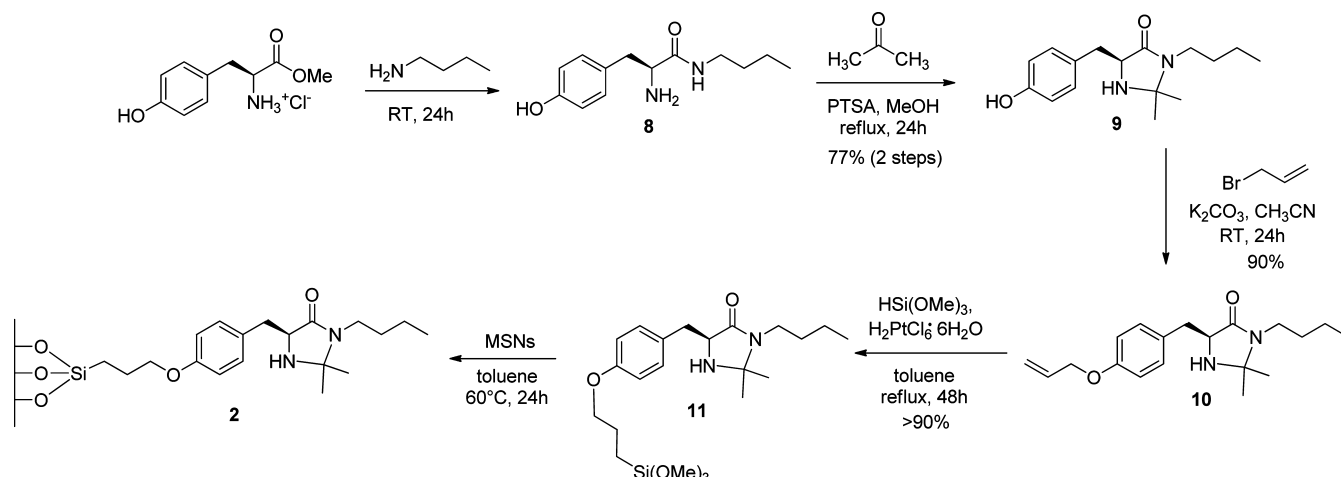
## RESULTS AND DISCUSSION

**Synthesis of the Silica-Supported Catalysts.** In designing the synthesis of silica-supported chiral imidazolidinones, we reasoned that, in principle, the most convenient route could involve the cocondensation of a silica precursor (namely TEOS, tetraethoxysilane) with a chiral organotrialkoxysilane bearing the imidazolidinone moiety; however, the drastic reaction conditions required for the cocondensation, in particular treatment of the siliceous material with HCl in MeOH at 60 °C, could lead to extensive degradation of the imidazolidinone ring. We therefore opted for a postgrafting functionalization of an already synthesized material with a chiral trialkoxysilane. With regard to the silica matrix, we chose to use mesoporous silica nanoparticles (MSNs) prepared from tetraethoxysilane in the presence of cetyltrimethylammonium bromide (CTAB) as the surfactant employed as templating agent.

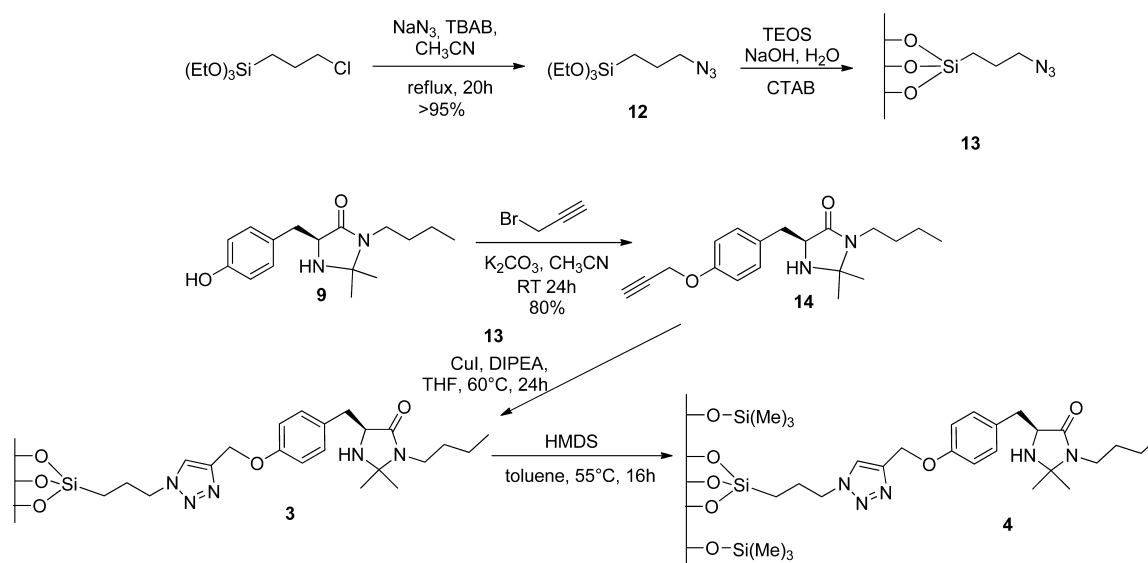
In principle, imidazolidin-4-ones such as MacMillan's first-generation catalysts offer two different sites for attachment to the solid support: the amide nitrogen at position 3 and the aryl residue at the stereogenic center (Figure 1).

Both opportunities were explored in this work: the condensation of allyl amine with (*S*)-phenylalanine methyl ester followed by an acid-catalyzed reaction with acetone afforded imidazolidinone **6** (Scheme 1) in 90% yield after one chromatographic purification.

Scheme 2. Synthesis of Supported Imidazolidinone 2



Scheme 3. Synthesis of Supported Azide 13 and Imidazolidinones 3 and 4



Platinum-catalyzed hydrosilylation with trimethoxysilane led to the enantiopure trialkoxysilane 7, which was grafted to mesoporous silica in toluene at 60 °C for 24 h to afford catalyst 1.

Another option is offered by the use of (*S*)-tyrosine instead of (*S*)-phenylalanine to generate an imidazolidinone already equipped with a properly located and chemically suitable handle for the heterogenization process.<sup>17</sup> Thus, starting from (*S*)-tyrosine methyl ester hydrochloride, imidazolidinone 9 was easily obtained in 77% yield by *N*-butyl amide formation and treatment with acetone (Scheme 2). Reaction with allyl bromide in acetonitrile in the presence of  $\text{Cs}_2\text{CO}_3$  allowed us to introduce the carbon–carbon double bond, instrumental for performing catalyst immobilization by platinum-catalyzed hydrosilylation. Grafting of the functionalized imidazolidinone 11 onto mesoporous silica nanoparticles (MSNs) in toluene at 60 °C for 24 h afforded the supported catalyst 2.

Preliminary experiments to assess the catalytic behavior of the immobilized catalysts 1 and 2 in the Diels–Alder cycloaddition between cinnamic aldehyde and cyclopentadiene<sup>18</sup> showed better performance for the latter (see the discussion of catalytic experiments); therefore, the study focused on the (*S*)-tyrosine-derived imidazolidinone and a different strategy to immobilize it was

investigated. Copper-catalyzed azide/alkyne dipolar cycloaddition was employed to connect the chiral catalyst to the properly derivatized siliceous material (Scheme 3). Siloxane 12 was readily prepared from commercially available (3-chloropropyl)-triethoxysilane and sodium azide in  $\text{CH}_3\text{CN}$  and was used in the cocondensation reaction with TEOS in the presence of CTAB to afford mesoporous silica-supported azide 13. Imidazolidinone 9 was reacted with propargyl bromide to afford derivative 14, which was subjected to copper-catalyzed cycloaddition with azide 13 to give catalyst 3. The latter was subjected to a capping reaction by treatment with hexamethyldisilazane to give catalyst 4, in order to evaluate if the free silanol groups on the silica surface could participate in the catalytic cycle by forming hydrogen bonds with the reagents.

**Characterization of Supported Catalysts.** <sup>13</sup>C and <sup>29</sup>Si MAS NMR. Solid-state <sup>29</sup>Si NMR experiments have been extensively used to characterize different surface incorporation patterns and conformations of siliceous material functionalized with organic residues. Nuclear magnetic resonance studies of silica-based materials are potentially useful, where applicable, since they provide well-resolved spectra that can easily characterize the bonding environment of silicon atoms near

the surface.<sup>19–21</sup> In this study, cross-polarization (CP) and direct-polarization (DP) magic angle spinning (MAS) <sup>13</sup>C and <sup>29</sup>Si NMR experiments were performed to investigate catalysts 1–4 in order to obtain evidence for the presence of the organic moieties in the mesoporous material and confirm their chemical structure. It is well recognized that a given surface silicon atom bearing a functional group can have a variable number *n* of Si–O–Si bonds, leading to so-called T<sub>1</sub>, T<sub>2</sub>, and T<sub>3</sub> substructures. The bonding schemes, for these hybrid materials containing organic functionalities, lead to very different geometries on the surface, as illustrated in Figure 2. Knowledge of the surface incorporation patterns and

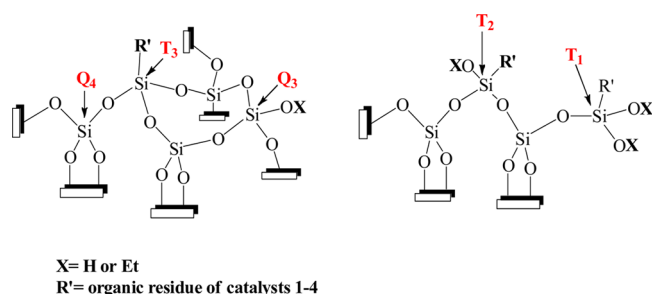


Figure 2. Possible Si substitution on the silica surface.

the conformations of functional groups for such materials is an essential step toward developing efficient functional substrates.

The <sup>29</sup>Si DP/MAS experiments, carried out according to previously described methods,<sup>21</sup> allowed us to perform quantitative measurements and determine the catalyst loading, providing the functionalization degree of the SiO<sub>2</sub> materials with the organic siloxane moieties. The <sup>29</sup>Si spectra gave also information about the bulk surface species Q<sub>4</sub> [(SiO)<sub>4</sub> Si] and proton-rich Q<sub>n</sub> sites: Q<sub>3</sub> [(SiO)<sub>3</sub> SiOH], Q<sub>2</sub> [(SiO)<sub>2</sub> Si(OH)<sub>2</sub>], and Q<sub>1</sub> [(SiO) Si(OH)<sub>3</sub>] (Figure 2).

The <sup>29</sup>Si solid-state spectra of catalysts 1–3 (Figure 3) are dominated by the resonance lines associated with the silicon sites Q<sub>4</sub>, Q<sub>3</sub>, and Q<sub>2</sub>. Moreover, the spectra clearly showed very different patterns for the functionalized T<sub>n</sub> species, where the silicon atoms are directly bound to at least one organic moiety.

The presence of peaks assigned to T<sub>3</sub>, T<sub>2</sub>, and T<sub>1</sub> showed that the organic groups are indeed covalently bound to the surface. Deconvolution analysis of <sup>29</sup>Si DP spectra of catalysts 1–3 were performed to recognize T<sub>n</sub> and Q<sub>n</sub> relative concentrations in order to determine the surface coverage (SC) and the molar concentrations of organic moieties, ranging from 0.62 to 1.43 mmol/g (for T<sub>n</sub> and Q<sub>n</sub> determinations, see the Supporting Information).

Finally, the <sup>13</sup>C spectra of catalysts 1–4 demonstrated that the mesopores were indeed functionalized as expected and the organic residues were stably bounded to the inorganic material (see the Supporting Information for details).

**Morphological Properties.** The morphological examination of the sample particles was performed by collecting images of the surfaces by SEM analysis. Figure 4 (left) shows the micrograph of azide 13, precursor of catalyst 3, at high magnification. As expected,<sup>16</sup> rod-shaped particles of different lengths and diameters (ca. 0.4 μm in length and 500 nm in diameter) with curved hexagonal-shaped tubular morphology completely cover irregular polyhedral-shaped grains, which can be associated with the silica morphology. Anchoring of the catalyst to the azido silica 13 did not deeply affect the morphology of the final particles. As can be seen by a SEM micrograph of the surface of 3 (Figure 4 right), an even more dense surface of rod-shaped tubular particles covers the silica grains which can now only be guessed (for more SEM images see the Supporting Information).

The textural properties in terms of surface areas, pore volumes, and pore size distributions of the azide 13 and catalyst

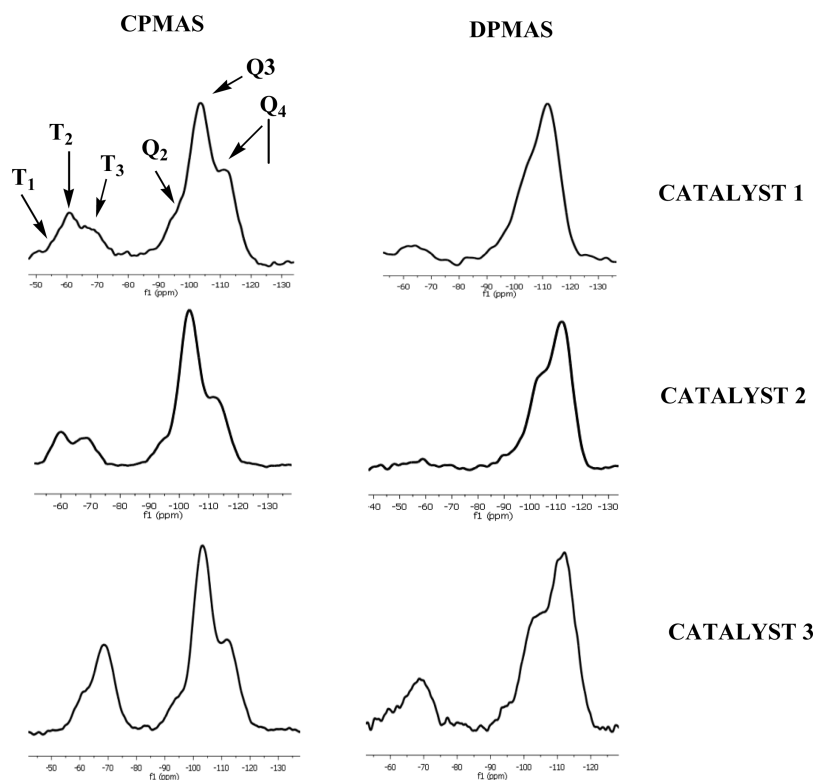


Figure 3. <sup>29</sup>Si CPMAS (left column) and DPMAS (right column) NMR spectra obtained for mesoporous catalysts 1–3.



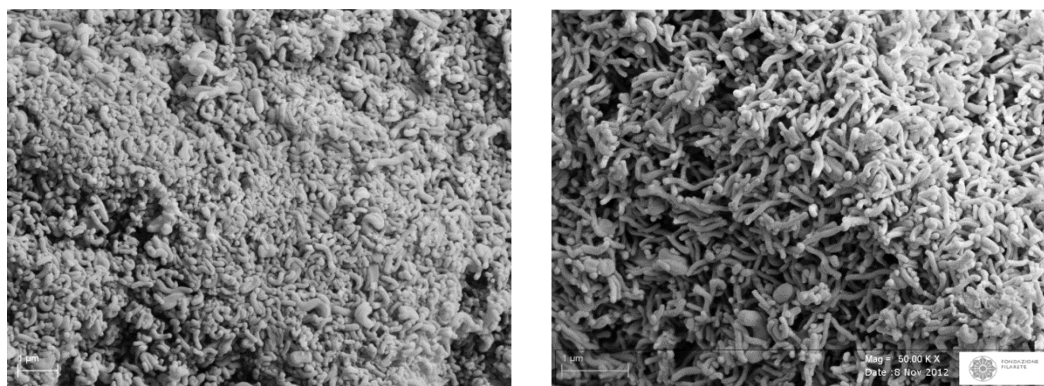


Figure 4. SEM images of a sample of the azide surface **13** (left) and of catalyst **3** (right) at magnifications of 10000 $\times$ .

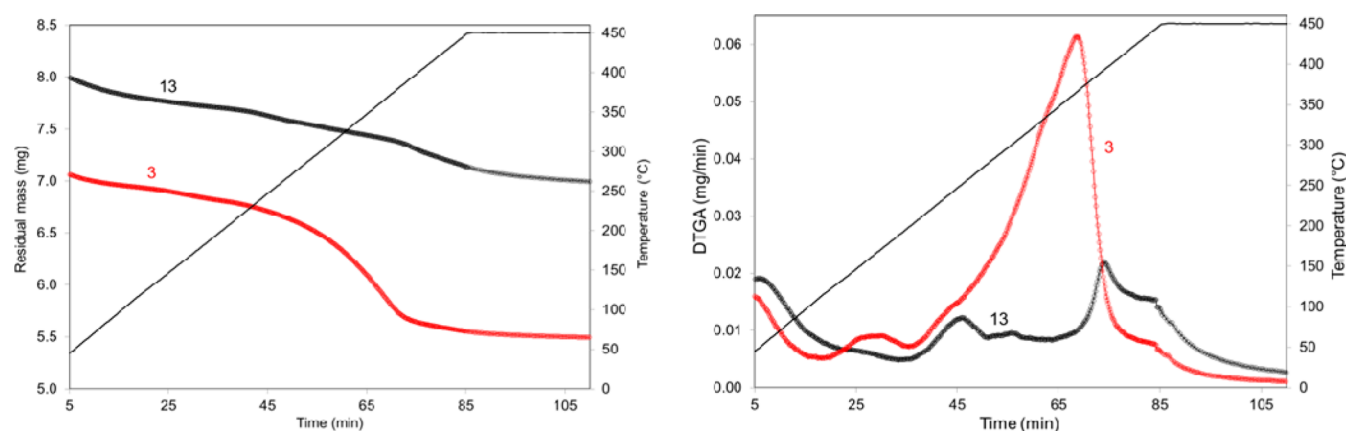


Figure 5. TGA (left) and DTGA (right) analysis of **13** and **3** samples. The linear rate increase (5 °C/min) used in the experiment is indicated on the right axis.

**3** have been determined by N<sub>2</sub> adsorption–desorption isotherms. The two surfaces have characteristic type IV BET isotherms consistent with the presence of cylindrical mesoscale pores. The BET surface areas of **13** and **3** are 1109 and 486.5 m<sup>2</sup> g<sup>-1</sup>, respectively. The loss of surface area observed for catalyst **3** could be due to the higher density of the organic functionalities loaded on the azide sample which completely cover the silica surface. The pore size distribution, calculated by the BJH approach, showed a defined pore population of sizes around 20 and 16 Å for **13** and **3**, respectively (see the Supporting Information for N<sub>2</sub> adsorption–desorption isotherms and calculated pore size BJH distribution curves).

In order to have an estimate of the total amount of the organic residues loaded on the silica surface, thermogravimetric analysis (TGA) was carried out under a linear increase rate of temperature (up to 450 °C) and in an air atmosphere to obtain the oxidative removal of all the organic residues bound to the silica surface. Figure 5 shows both the thermograms obtained in terms of residual mass as a function of time and the derivative of the mass loss, the DTGA curves, for samples **13** and **3**.

For both samples **3** and **13** an initial mass loss likely associated with the desorption of some water and organic species from the silica surface could be observed. Azide **13** showed two transitions at 246 and 390 °C with a total mass loss of 10.9% (estimated between 100 and 450 °C temperature interval); the calculated amount of organic residue removed was 1.29 mmol/g of silica. Catalyst **3** showed a first transition at 159 °C followed by a very intense transition at 364 °C, with a very broad and high peak leading to a total mass loss of 21.12%.

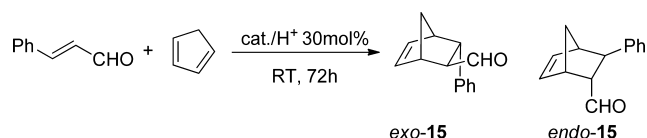
Although at the moment there is no single reliable analytical technique for the quantification of different organic residues on silica matrices, by using a combination of several methods it is possible to gain detailed information about functionalized materials. In particular, well-established analytical techniques such as MAS NMR could be used not only to characterize different surface incorporation patterns but also to determine the ratio between two different organic residues.

#### Catalytic Behavior of the Immobilized Catalysts.

Catalysts **1–4** were tested in the Diels–Alder reaction between cinnamic aldehyde (1 equiv) and cyclopentadiene (5 equiv) in MeOH/H<sub>2</sub>O or CH<sub>3</sub>CN/H<sub>2</sub>O at room temperature for 72 h using 30 mol % of the supported catalyst.<sup>22</sup> HBF<sub>4</sub> was added to the reaction mixture in order to protonate the imidazolidinone and generate the actual catalytic species.<sup>10b</sup> The results are summarized in Table 1.

Catalyst **1** afforded cycloadducts **15** in 74% yield with 72% ee for the *endo* isomer and 76% ee for the *exo* isomer (Table 1, entry 1); catalyst **2** performed comparably in terms of stereochemical activity (76% ee for the *exo* isomer) but much better in terms of chemical activity, affording the cycloadducts quantitatively (entry 3). Since preforming the catalyst led to a marked decrease of both yield and stereoselection (entry 2), the in situ addition of HBF<sub>4</sub> was preferred. Use of trifluoroacetic acid (TFA) as protonating agent led to improved stereoselectivity (81% ee for the *endo* isomer and 78% ee for the *exo* isomer) and lower yield (entry 5) in CH<sub>3</sub>CN/H<sub>2</sub>O as solvent. Catalysts derived from the copper-catalyzed azide–alkyne cycloaddition (catalysts **3** and **4**) performed better than their grafted

Table 1. Diels–Alder Reactions Promoted by Catalysts 1–4



entry	catalyst	solvent	yield (%) <sup>a</sup>	endo:exo <sup>b</sup>	endo, exo ee (%) <sup>c</sup>
1	1	MeOH/H <sub>2</sub> O 95/5	74	56:44	72, 76
2 <sup>d</sup>	1	MeOH/H <sub>2</sub> O 95/5	27	53:47	42, 61
3	2	MeOH/H <sub>2</sub> O 95/5	98	28:72	58, 76
4	2	CH <sub>3</sub> CN/H <sub>2</sub> O 95/5	84	55:45	66, 70
5 <sup>e</sup>	2	CH <sub>3</sub> CN/H <sub>2</sub> O 95/5	70	55:45	81, 78
6	3	MeOH/H <sub>2</sub> O 95/5	66	56:44	88, 90
7 <sup>e</sup>	3	MeOH/H <sub>2</sub> O 95/5	98	56:44	87, 80
8	4	MeOH/H <sub>2</sub> O 95/5	66	56:44	84, 91
9	3	CH <sub>3</sub> CN/H <sub>2</sub> O 95/5	75	55:45	91, 89
10 <sup>f</sup>	3	CH <sub>3</sub> CN/H <sub>2</sub> O 95/5	91	55:45	92, 90

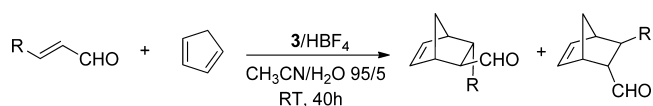
<sup>a</sup>Isolated yield after chromatographic purification. <sup>b</sup>Evaluated by <sup>1</sup>H NMR on the crude reaction mixture. <sup>c</sup>Evaluated by HPLC and GC on a chiral stationary phase after reduction to the corresponding alcohol. <sup>d</sup>The protonated catalyst was isolated and then used in the reaction. <sup>e</sup>Trifluoroacetic acid was used. <sup>f</sup>The reaction was set using 5 equiv of cyclopentadiene; after 20 h, 5 equiv of cyclopentadiene was added for a total reaction time of 40 h.

counterparts. Catalyst 3 afforded the cycloadducts in 66% yield with 88% ee for the *endo* isomer and 90% ee for the *exo* isomer (entry 6), results comparable to those obtained by the nonsupported chiral imidazolidinone;<sup>18</sup> using 3/TFA resulted in an increase of the chemical yield but an erosion of the enantiomeric excess (entry 7 vs entry 6). Capped catalyst 4 performed equally well in comparison to catalyst 3 (entry 8), giving the products with 66% yield and 84% ee for the *endo* isomer and 91% ee for the *exo* isomer, pointing out that the free silanol groups on the silica surface did not alter the catalytic efficiency of the imidazolidinone. Using catalyst 3/HBF<sub>4</sub> in CH<sub>3</sub>CN/H<sub>2</sub>O as the solvent system allowed us to improve both yield and stereoselection, affording the products in 75% yield and 91% ee for the *endo* isomer and 89% ee for the *exo* isomer (entry 9 vs entry 6). By slightly changing the reaction conditions, that is by adding 5 equiv more of cyclopentadiene after 20 h, we were able to improve the catalytic efficiency and shorten the reaction time, obtaining the cycloadducts in quantitative yield, with 92% ee for the *endo* isomer and 90% ee for the *exo* isomer in 40 h (entry 10).

Having thus established the best reaction conditions (entry 10), we extended the scope of the Diels–Alder reaction to differently substituted aldehydes. The results are summarized in Table 2.

Reaction with an aliphatic aldehyde such as crotonic aldehyde afforded the cycloadducts in quantitative yield with 78% ee for the *endo* isomer and 76% ee for the *exo* isomer (Table 2, entry 1). 4-Bromocinnamic aldehyde reacted with cyclopentadiene to afford the products in high yield (94%) and high enantiomeric excess (88% and 85% for the *endo* and *exo* isomers, respectively) (entry 2). Catalyst 3/HBF<sub>4</sub> promoted the reaction between electron-deficient 4-nitrocinnamic aldehyde and cyclopentadiene with 92% yield and 91% ee for the *endo* isomer and 87% ee for the *exo* isomer (entry 3) and also between the more sterically demanding 2-nitrocinnamic aldehyde and cyclopentadiene, affording the cycloadducts with 92% yield and 91% ee for the *endo* isomer and 84% ee for the *exo* isomer (entry 4).

Table 2. Diels–Alder Reaction between Cyclopentadiene and Different Aldehydes



entry	R	yield (%) <sup>a</sup>	endo:exo <sup>b</sup>	endo, exo ee (%) <sup>c</sup>
1	CH <sub>3</sub>	98	41:59	78, 76
2	4-Br-Ph	84	50:50	88, 85
3	4-NO <sub>2</sub> -Ph	92	50:50	91, 87
4	2-NO <sub>2</sub> -Ph	92	45:55	91, 84

<sup>a</sup>Isolated yield after chromatographic purification. <sup>b</sup>Evaluated by <sup>1</sup>H NMR on the crude reaction mixture. <sup>c</sup>Evaluated by HPLC or GC on a chiral stationary phase after reduction to the corresponding alcohol.

One of the main goals of supporting a catalyst onto a solid matrix is to facilitate its recovery and recyclability. The anchoring of an organic catalyst onto silica offers the opportunity of recovering the catalytic species by simple separation from the crude reaction mixture using filtration or centrifugation. After a Diels–Alder reaction between cyclopentadiene and cinnamic aldehyde, catalyst 3 was recovered by centrifugation, washed with CH<sub>2</sub>Cl<sub>2</sub>/MeOH, dried for 3 h at 60 °C under high vacuum, and reused in the next reaction after activation with HBF<sub>4</sub>. Results of this iterative procedure are reported in Table 3.

Table 3. Recycling Experiments of Catalyst 3

entry	yield (%) <sup>a</sup>	endo:exo <sup>b</sup>	endo, exo ee (%) <sup>c</sup>
1	91	55:45	92, 90
2	63	55:45	87, 83
3	41	55:45	72, 74

<sup>a</sup>Isolated yield after chromatographic purification. <sup>b</sup>Evaluated by <sup>1</sup>H NMR on the crude reaction mixture. <sup>c</sup>Evaluated by HPLC on a chiral stationary phase after reduction to the corresponding alcohol.

The cycloadducts were obtained in decreasing yields (63% and 41% in the second and third runs, respectively) and decreasing enantiomeric excesses (87% and 72% for the *endo* isomer in the second and third runs, respectively). When the catalyst was employed in a fourth run, no product was obtained.<sup>23</sup> While the diminished chemical activity was somehow predictable, although more cycles were usually possible with different supported imidazolidinones, the loss of stereochemical activity was more surprising.<sup>10</sup> Table 4 reports some recycling data of different supported chiral imidazolidinones in the Diels–Alder cycloaddition between cyclopentadiene and  $\alpha,\beta$ -unsaturated aldehydes. Poly(ethylene glycol)-supported imidazolidinone 16 (Figure 6) could be recovered from the reaction mixture between cyclopentadiene and acrolein (67% yield, 92% ee; entry 3, Table 4) and reused in a second cycle to afford the product in 61% yield, and 87% ee; iteration of the recovery/recycling protocol was possible for two more cycles, both occurring with almost unchanged stereoselectivities (87% and 85% ee, respectively) but decreasing yields (50% and 38%, respectively). When the catalyst was used in a fifth cycle, the yield was very low (10–15% after 60 h).<sup>10a</sup> More recently, our group reported the use of poly(methylhydrosiloxane)-supported chiral imidazolidinone 17, which could be reused five times in the Diels–Alder cycloaddition between cyclopentadiene and cinnamic aldehyde with only marginal loss of chemical activity (yield from 65% to 53%, entries 5 and 6) and with no appreciable decrease of stereo- and enantiocontrol, affording both *exo* and *endo*

**Table 4.** Comparison of Supported Catalysts **3** and **16–18** in the Synthesis of Adducts **15**

entry	catalyst	support	run	yield (%)	endo ee (%)
1	<b>3</b> /HBF <sub>4</sub>	MSNs	1	91	92
2			3	41	72
3 <sup>a</sup>	<b>16</b> /TFA	PEG	1	67	92
4 <sup>a</sup>			4	38	85
5	<b>17</b> /HBF <sub>4</sub>	PMHS	1	65	93
6			6	53	91
7	<b>18</b> /TFA	PMO	1	98	81
8			8	86	78

<sup>a</sup>Acrolein instead of cinnamic aldehyde was used.

isomers with enantioselectivity always higher than 90%.<sup>10b</sup> Finally, Wang and co-workers showed that hollow periodic mesoporous organosilica spheres functionalized with MacMillan imidazolidinone **18** could be reused for at least seven runs in the Diels–Alder cycloaddition between cyclopentadiene and cinnamic aldehyde without a noticeable decrease in enantioselectivity (from 81% ee to 78% ee, entries 7 and 8), although with some loss of the reaction yield (from 98% to 86%).<sup>14</sup>

We reasoned that the difficulty in recovering and recycling catalyst **3** could be ascribed not only to some degradation of the imidazolidinone moiety (as demonstrated elsewhere<sup>17</sup>) but also to degradation of the silica network, which can be sensitive to mechanical stress. It seems possible that extensive manipulations of the catalyst, such as the repeated cycles of washing, stirring, centrifugation, and filtration could ultimately lead to a collapse of the organic–inorganic silica network, thus limiting the recyclability of the catalyst. Since we have no evidence at the moment for supporting our hypothesis, further studies are currently underway toward a better understanding of the mechanical properties of the MSNs; in order to avoid grinding of the material, the use of an orbital shaker during the catalytic test instead of the common magnetic stirring is programmed.<sup>24</sup>

## CONCLUSIONS

The synthesis of four imidazolidinones supported on mesoporous silica nanoparticles was reported. The catalysts were extensively characterized by different analytical techniques: <sup>29</sup>Si and <sup>13</sup>C MAS NMR for structural confirmation and silicon atom substitution, and N<sub>2</sub> physisorption, SEM, and

TGA in order to evaluate structural and morphological properties. Catalysts **1–4** were tested in the Diels–Alder cycloaddition between cyclopentadiene and cinnamic aldehyde; catalyst **3** proved to be the most efficient, affording the product in yield and enantiomeric excess comparable to those obtained by using nonsupported chiral imidazolidinones. The scope of the reaction was also extended to different substituted aldehydes. Attempts to recover and recycle the catalyst showed some limitations of the system but offered the opportunity to get some insights into the stability of the silica network.

## EXPERIMENTAL SECTION

**Materials.** Dichloro(dicyclopentadienyl)platinum(II) (dcpPtCl<sub>2</sub>; Aldrich 97%) was purchased from Sigma-Aldrich and used without further purification.

All reactions were carried out in oven-dried glassware with magnetic stirring under a nitrogen atmosphere, unless otherwise stated. Dry solvents were purchased and stored under nitrogen over molecular sieves (bottles with crown caps). Reactions were monitored by analytical thin-layer chromatography (TLC) using silica gel 60 F<sub>254</sub> precoated glass plates (0.25 mm thickness) and visualized using UV light or phosphomolybdic acid.

**NMR Spectroscopy.** The <sup>1</sup>H and <sup>13</sup>C NMR spectra were recorded at 500.0 and 125.62 MHz, respectively. The spectra were measured with CDCl<sub>3</sub> as solvent and the chemical shifts externally referenced to TMS.

**Solid-State NMR.** The <sup>13</sup>C and <sup>29</sup>Si solid-state NMR spectra were recorded at 125.62 and 99.36 MHz, respectively, on a Bruker Avance 500 spectrometer, equipped with a 4 mm magic angle spinning (MAS) broad-band probe (spinning rate  $\nu_R$  up to 13 kHz). The MAS spectra were performed on solid samples, (typically 0.12 g); each sample was packed into a 4 mm MAS rotor (50  $\mu$ L sample volume) spinning at 13 kHz at a temperature of 300 K. Direct polarization (DP) and variable amplitude cross-polarization (CP) methods (contact time  $\tau_c$  1 ms) were used for recording the <sup>29</sup>Si spectra with 400 scans and a delay of 300.0 and 20000 scans and a delay of 3.0 s, respectively. The <sup>13</sup>C experiments were performed with the CP method using a contact time  $\tau_c$  of 1.5 ms, 70000 scans, and 3.0 s of delay. All chemical shifts were externally referenced to TMS.

The <sup>29</sup>Si resonances were assigned following previous reports in the literature,<sup>21</sup> while those of <sup>13</sup>C were referenced to the chemical shifts found in the solution spectra of the corresponding unbound compounds.

**N<sub>2</sub> Physisorption.** Sample surface area (m<sup>2</sup> g<sup>-1</sup>), pore volume (cm<sup>3</sup> g<sup>-1</sup>), and pore size distribution were determined from N<sub>2</sub> adsorption and desorption isotherms measured at liquid nitrogen temperature with an automatic surface area analyzer; the BET and BJH methods were employed for the computations. Prior to the

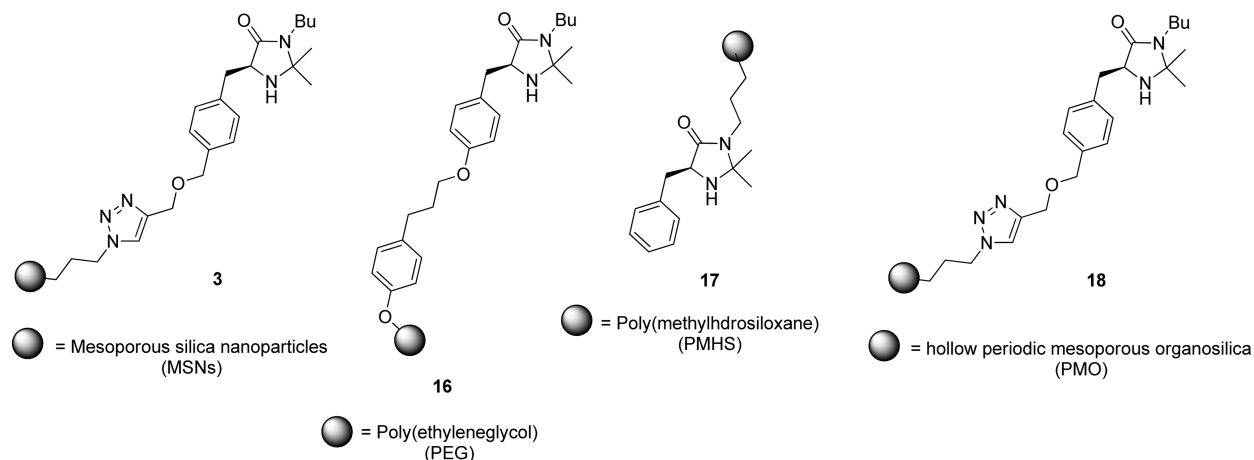


**Figure 6.** Supported chiral imidazolidinones.



measurement, the sample (ca. 1 g), crushed and sieved as 0.250–0.354 mm particles, was thermally activated at 90 °C for 4 h under vacuum. The pore volume was determined from the total amount of N<sub>2</sub> adsorbed at  $P/P_0 = 0.95$  using the N<sub>2</sub> density in the normal liquid state ( $\rho = 0.8081 \text{ g cm}^{-3}$ ); the N<sub>2</sub> molecular area was taken as 16.2 Å<sup>2</sup>. The pore size distribution was obtained by the BJH (Barrer, Joyner, and Halenda) model equation on the basis of the desorption branch of the N<sub>2</sub> isotherm.

**Thermogravimetry.** Thermogravimetric analysis (TGA) was performed on dried samples in the temperature interval from 50 to 450 °C under flowing air with a ramp of 5 °C min<sup>-1</sup> and maintaining the final temperature for 30 min.

**Scanning Electron Microscopy.** Scanning electron micrographs (SEM) were obtained by a FE-SEM instrument operating at 0.2–30 kV. The powder samples were coated with gold before analysis.

Compounds 5, 6, 8–10, 12, and 14 were prepared according to published procedures.<sup>10,17,25</sup>

**Compound 7.** To a solution of imidazolidinone 6 (2.84 g, 11.7 mmol) in THF (30 mL) were added trimethoxysilane (4.5 mL, 35 mmol) and dcpPtCl<sub>2</sub> (48 mg 0.12 mmol), in that order. The mixture was refluxed under nitrogen for 24 h; the solvent was evaporated, and the crude imidazolidinone 7 was obtained in quantitative yield as a brown oil and used without further purification. <sup>1</sup>H NMR (500 MHz, CDCl<sub>3</sub>, 25 °C, TMS):  $\delta$  7.28 (t, <sup>3</sup>J(H,H) = 7.5 Hz, 2H), 7.22 (m, 3H), 3.76 (t, <sup>3</sup>J(H,H) = 5 Hz, 1H), 3.6 (s, 9H), 3.3 (part B of an AB system, 1H), 3.05 (m, 2H), 2.9 (part A of an AB system, 1H), 1.55 (m, 2H), 1.25 (s, 3H), 1.15 (s, 3H), 0.6 ppm (t, <sup>3</sup>J(H,H) = 7.4 Hz, 2H). <sup>13</sup>C NMR (125 MHz, CDCl<sub>3</sub>, 25 °C, TMS):  $\delta$  173.8, 137.0, 129.6, 128.5, 126.8, 76.0, 58.8, 50.5, 42.8, 37.0, 28.0, 26.5, 22.4, 6.6 ppm.

**Compound 11.** To a solution of imidazolidinone 10 (1.1 g, 3.47 mmol) in THF (10 mL) were added trimethoxysilane (1.3 mL, 10.4 mmol) and dcpPtCl<sub>2</sub> (12 mg 0.03 mmol), in that order. The mixture was refluxed under nitrogen for 24 h; the solvent was evaporated, and the crude imidazolidinone 11 was obtained in quantitative yield as a brown oil and used without further purification. <sup>1</sup>H NMR (500 MHz, CDCl<sub>3</sub>, 25 °C, TMS):  $\delta$  7.07 (d, <sup>3</sup>J(H,H) = 8.3 Hz, 2H), 6.77 (d, <sup>3</sup>J(H,H) = 8.3 Hz, 2H), 3.85 (t, <sup>3</sup>J(H,H) = 7.9 Hz, 2H), 3.66 (dd, <sup>3</sup>J(H,H) = 5.5 and 4.6 Hz, 1H), 3.51 (s, 9H), 3.28 (part B of an AB system, 1H), 3.05 (AB system, <sup>3</sup>J(H,H) = 11.0, 5.5, and 4.6 Hz, 2H), 2.85 (part A of an AB system, 1H), 1.83 (qui, <sup>3</sup>J(H,H) = 7.9 Hz, 2H), 1.40 (m, 2H), 1.25 (m, 2H), 1.22 (s, 3H), 1.10 (s, 3H), 0.87 (t, <sup>3</sup>J(H,H) = 7.9 Hz, 3H), 0.74 ppm (t, <sup>3</sup>J(H,H) = 7.9 Hz, 2H). <sup>13</sup>C NMR (125 MHz, CDCl<sub>3</sub>, 25 °C, TMS):  $\delta$  173.9, 158.0, 130.6, 128.4, 114.5, 76.0, 69.6, 58.8, 50.4, 40.2, 35.7, 31.3, 27.9, 26.4, 22.4, 20.3, 13.7, 5.2 ppm.

**General Procedure for the Synthesis of MSNs.** A solution of cetyltrimethylammonium bromide (365 mg, 1 mmol) in water (88 mL) and 2 M NaOH (1.3 mL) was mechanically stirred at 550 rpm at 80 °C for 30 min. The stirring speed was decreased to 200 rpm, and tetraethoxysilane (TEOS, 1.82 mL, 8.16 mmol) was rapidly added. In the case of a functionalized material the properly modified organotrialkoxysilane (1.05 mmol) was added with TEOS. After 2 min of stirring at 200 rpm a precipitate was formed. Stirring at 500–600 rpm was continued for 2.0 h at 80 °C, and the mixture was filtered while still hot. The solid was washed with water (150 mL) and MeOH (150 mL) and dried under high vacuum for 3 h to afford a white material (794 mg). This was then treated with a solution of concentrated HCl (0.6 mL) in MeOH (80 mL) under mechanical stirring for 2.5 h at 60 °C in order to remove the surfactant. The cooled mixture was filtered and the solid washed again with water and MeOH (100 mL each). The white solid was dried under high vacuum for 3 h at 90 °C and subjected to an alkaline wash with a saturated Na<sub>2</sub>CO<sub>3</sub> methanol solution (100 mL/g). After 3 h of stirring at 550 rpm at room temperature the mixture was filtered and the solid was washed with water and methanol and dried under high vacuum at 80 °C for 3 h. The material was finally suspended in distilled water (100 mL/g) and mechanically stirred at 550 rpm at room temperature for 2 h, filtered on a porous septum, washed with methanol, and dried under high vacuum at 60 °C to constant weight.

**Compound 13.** This compound was prepared according to the general procedure for the synthesis of MSNs by co-condensation of azide 12 with TEOS.

**General Procedure for Grafting Reaction (Catalysts 1 and 2).** MSNs (1 g) and the properly modified organotrimethoxysilane (2 mmol) were suspended in toluene (10 mL) and stirred under an inert atmosphere at reflux for 48 h. The catalyst was isolated by centrifugation, washed with CH<sub>2</sub>Cl<sub>2</sub> (2 × 10 mL), and dried under vacuum.

**Catalyst 3.** To a solution of compound 14 (1.47 g, 4.68 mmol) in tetrahydrofuran (40 mL) were sequentially added *N,N*-diisopropylethylamine (8.2 mL, 46.8 mmol), copper(I) iodide (10 mg, 0.05 mmol), and azide 13 (3 g), in that order. The mixture was stirred at 35 °C for 40 h, and then it was centrifuged and the residue was washed three times with a dichloromethane/methanol mixture (9/1, v/v).

After centrifugation the solid was recovered and dried under high vacuum to constant weight.

**Catalyst 4.** To a suspension of catalyst 3 (1 g) in toluene (6 mL) was added hexamethyldisilazane (0.42 mL), and the mixture was stirred at 85 °C. After 18 h it was filtered and the solid residue was washed sequentially with toluene, methanol, and acetone and dried under high vacuum to constant weight.

**General Procedure for Diels–Alder Cycloaddition between Cyclopentadiene and Cinnamic Aldehyde (Compound 15).** To a suspension of the catalyst (30 mol %) in the solvent mixture (2 mL of 95/5 acetonitrile/water, v/v) was added tetrafluoroboric acid solution (48 wt % in water, stoichiometric to the catalyst), and the mixture was stirred for 10 min. Freshly distilled *trans*-cinnamic aldehyde (0.26 mmol, 33  $\mu$ L) and cyclopentadiene (1.3 mmol, 107  $\mu$ L) were added sequentially, and the mixture was stirred at room temperature for 20 h. Freshly distilled cyclopentadiene (1.3 mmol, 107  $\mu$ L) was added again, and the mixture was stirred for a further 20 h. After this reaction time, the mixture was centrifuged and the residue was washed with dichloromethane (2 × 10 mL). After centrifugation the heterogeneous catalyst was recovered and dried under high vacuum at 60 °C for 3 h. The supernatants were concentrated under vacuum, and <sup>1</sup>H NMR of the crude product was performed in order to evaluate the conversion and the *endo:exo* ratio. The *endo:exo* ratio was determined by using the CHO signals at  $\delta$  9.60 (*endo*) and 9.93 (*exo*) ppm.

If it was clean enough, the crude product (yellow oil) was dissolved in 2 mL of methanol and reduced with NaBH<sub>4</sub> (2 equiv). The mixture was stirred at room temperature for 1 h, and then 1 mL of distilled water was added. The mixture was extracted with dichloromethane (3 × 5 mL) and then concentrated under vacuum to afford the alcohol. This product is known and was purified by flash column chromatography on silica gel with a 90/10 hexane/ethyl acetate mixture as eluent, affording a mixture of *endo* and *exo* Diels–Alder adducts.

Data for the *endo* product are as follows.  $R_f = 0.42$  (hex/EtOAc 9/1 stained blue with phosphomolybdic acid). <sup>1</sup>H NMR (300 MHz, CDCl<sub>3</sub>):  $\delta$  9.61 (d,  $J = 2.2$  Hz, 1H), 7.14–7.34 (m, 5H), 6.43 (dd,  $J = 3.3, 5.6$  Hz, 1H), 6.18 (dd,  $J = 2.8, 5.7$  Hz, 1H), 3.34 (brs, 1H), 3.14 (brs, 1H), 3.10 (d,  $J = 4.8$ , 1H), 2.99 (dd,  $J = 2.7, 5.4$ , 1H), 1.82 (d,  $J = 8.7$ , 1H), 1.61–1.64 (m, 1H). Data for the *exo* product are as follows.  $R_f = 0.42$  (hex/EtOAc 9/1 stained blue with phosphomolybdic acid). <sup>1</sup>H NMR (300 MHz, CDCl<sub>3</sub>):  $\delta$  9.93 (d,  $J = 2.0$  Hz, 1H), 7.14–7.34 (m, 5H), 6.34 (dd,  $J = 3.4, 5.5$  Hz, 1H), 6.08 (dd,  $J = 3.0, 5.5$  Hz, 1H), 3.73 (t,  $J = 3.8$ , 1H), 3.23 (m, 2H), 2.60 (dd,  $J = 1.5, 3.4$ , 1H), 1.61–1.64 (m, 2H).

**Synthesis of ((1*S*,2*S*,3*S*,4*R*)-3-Phenylbicyclo[2.2.1]hept-5-en-2-yl)methanol and ((1*R*,2*S*,3*S*,4*S*)-3-Phenylbicyclo[2.2.1]hept-5-en-2-yl)methanol.** Data for an *endo/exo* mixture are as follows. <sup>1</sup>H NMR (300 MHz, CDCl<sub>3</sub>):  $\delta$  7.18–7.31 (m, 10H), 6.34–6.41 (m, 2H), 6.15–6.20 (m, 1H), 5.93–5.98 (m, 1H), 3.86–3.94 (m, 1H), 3.59–3.70 (m, 3H), 3.39 (t,  $J = 12.8$  Hz, 1H), 3.04 (br s, 2H), 2.83–2.88 (m, 3H), 2.30–2.42 (m, 2H), 2.15–2.18 (m, 2H), 1.76–1.82 (d,  $J = 8.9$ , 1H), 1.65–1.68 (d,  $J = 8.7$ , 1H). The enantiomeric excess was determined by chiral HPLC with a Daicel Chiralcel OJ-H column (eluent 7/3 hex/IPA; 0.8 mL/min flow rate, detection 225 nm):  $t_R$  11.6 min (*endo*, minor),  $t_R$  23.9 min (*endo*, major),  $t_R$  30.3 min (*exo*, minor),  $t_R$  40.3 min (*exo*, major).



## ■ ASSOCIATED CONTENT

### ■ Supporting Information

Text, figures, and tables giving  $^{13}\text{C}$  and  $^{29}\text{Si}$  MAS NMR of catalysts 1–4, BET isotherms and BJH distributions of compounds 3 and 13, NMR and HPLC spectra of the cycloadducts, and SEM images of bare silica and catalyst 2. This material is available free of charge via the Internet at <http://pubs.acs.org>.

## ■ AUTHOR INFORMATION

### Corresponding Author

\*E-mail for A.P.: [alessandra.puglisi@unimi.it](mailto:alessandra.puglisi@unimi.it).

### Notes

The authors declare no competing financial interest.

## ■ ACKNOWLEDGMENTS

This paper is dedicated to Professor Maurizio Prato on the occasion of his 60th birthday. This work was supported by the MIUR-PRIN (Nuovi metodi catalitici stereoselettivi e sintesi stereoselettiva di molecole funzionali), Cariplo Foundation (Milano) within the project 2011-0293 “Novel chiral recyclable catalysts for one-pot, multi-step synthesis of structurally complex molecules”, and FIRB project RBF10BF5 V “Multifunctional hybrid materials for the development of sustainable catalytic processes”. M.B. thanks the COST action CM9505 “ORCA” Organocatalysis.

## ■ REFERENCES

- (1) (a) Nefzi, A.; Ostresh, J. M.; Houghten, R. A. *Chem. Rev.* **1997**, *97*, 449. (b) Plante, O. J.; Palmacci, E. R.; Seeberger, P. H. *Science* **2001**, *291*, 1523. (c) Myers, R. M.; Roper, K. A.; Baxendale, I. R.; Ley, S. V. The evolution of immobilised reagents and their application in flow chemistry for the synthesis of natural products and pharmaceutical compounds. In *Modern Tools for the Synthesis of Complex Bioactive Molecules*; Cossy, J., Arseniyadis, S., Eds.; Wiley: New York, 2012; pp 359–394. (d) Baxendale, I. R.; Ley, S. V. Heterogeneous Reactions. In *New Avenues to Efficient Chemical Synthesis, Emerging Technologies*; Seeberger, P. H., Blume, T., Eds.; Springer-Verlag: Berlin/Heidelberg, 2007; pp 151–185. (e) *Solid-Phase Organic Synthesis: Concepts, Strategies, and Applications*; Toy, P. H., Lam, Y., Eds.; Wiley: New York, 2012.
- (2) Lee, A.; Breitenbucher, J. G. *Curr. Opin. Drug Discovery Dev.* **2003**, *6*, 494.
- (3) Jas, G.; Kirschning, A. *Chem. Eur. J.* **2003**, *9*, 5708.
- (4) Solinas, A.; Taddei, M. *Synthesis* **2007**, 2409.
- (5) Kirschning, A.; Solodenko, W.; Mennecke, K. *Chem. Eur. J.* **2006**, *12*, 5972.
- (6) Trindade, A. F.; Afonso, C. A. M. *Chem. Rev.* **2009**, *109*, 3401.
- (7) (a) *Recoverable and Recyclable Catalysts*; Benaglia, M., Ed.; Wiley: Chichester, U.K., 2009. (b) Haraguchi, N.; Itsuno, S. *Polymeric Chiral Catalyst Design and Chiral Polymer Synthesis*; Wiley: Chichester, U.K., 2011. (c) *Handbook of Asymmetric Heterogeneous Catalysts*; Ding, K. J., Uozomi, F. J. K., Eds.; Wiley-VCH: Weinheim, Germany, 2008.
- (8) Reviews on supported organic catalysts: (a) Benaglia, M.; Puglisi, A.; Cozzi, F. *Chem. Rev.* **2003**, *103*, 3401. (b) Cozzi, F. *Adv. Synth. Catal.* **2006**, *348*, 1367. (c) Benaglia, M. *New J. Chem.* **2006**, *30*, 1525.
- (9) Lelais, G.; MacMillan, D. W. C. *Aldrichim. Acta* **2006**, *39*, 79.
- (10) (a) Benaglia, M.; Celentano, G.; Cinquini, M.; Puglisi, A.; Cozzi, F. *Adv. Synth. Catal.* **2002**, *344*, 149. (b) Guizzetti, S.; Benaglia, M.; Siegel, J. S. *Chem. Commun.* **2012**, *48*, 3188.
- (11) Selkälä, S. A.; Tois, J.; Pihko, P. M.; Koskinen, A. M. P. *Adv. Synth. Catal.* **2002**, *344*, 941.
- (12) Zhang, Y.; Zhao, L.; Lee, S. S.; Ying, J. Y. *Adv. Synth. Catal.* **2006**, *348*, 2027.
- (13) Hagiwara, H.; Kuroda, T.; Hoshi, T.; Suzuki, T. *Adv. Synth. Catal.* **2010**, *352*, 909.

(14) (a) Shi, J. Y.; Wang, C. A.; Li, Z. J.; Wang, Q.; Zhang, Y.; Wang, W. *Chem. Eur. J.* **2011**, *17*, 6206. (b) Riente, P.; Yadav, J.; Pericas, M. A. *Org. Lett.* **2012**, *14*, 3668.

(15) (a) Dickschat, A. T.; Behrends, F.; Surmiak, S.; Weiß, M.; Eckert, H.; Studer, A. *Chem. Commun.* **2013**, *49*, 2195. (b) Dickschat, A. T.; Behrends, F.; Bühner, M.; Ren, J.; Weiß, M.; Eckert, H.; Studer, A. *Chem. Eur. J.* **2012**, *18*, 16689. (c) Nakazawa, J.; Smith, B. J.; Stack, T. D. P. *J. Am. Chem. Soc.* **2012**, *134*, 2750.

(16) Puglisi, A.; Annunziata, R.; Benaglia, M.; Cozzi, F.; Gervasini, A.; Bertacche, V.; Sala, M. C. *Adv. Synth. Catal.* **2009**, *351*, 219.

(17) See ref 10 and also: Puglisi, A.; Benaglia, M.; Cinquini, M.; Cozzi, F.; Celentano, G. *Eur. J. Org. Chem.* **2004**, 567.

(18) Ahrendt, K. A.; Borths, C. J.; MacMillan, D. W. C. *J. Am. Chem. Soc.* **2000**, *122*, 4243.

(19) Asefa, T.; MacLachlan, M. J.; Coombs, N.; Ozin, G. A. *Nature* **1999**, *402*, 867.

(20) Athens, G. L.; Shayib, R. M.; Chmelka, B. F. *Curr. Opin. Colloid Interface Sci.* **2009**, *14*, 281.

(21) (a) Huh, S.; Wiench, J. W.; Ji-Chul, Y.; Pruski, M.; Lin, V. S.-Y. *Chem. Mater.* **2003**, *15*, 4247. (b) Huh, S.; Chen, H.-T.; Wiench, J. W.; Pruski, M.; Lin, V. S.-Y. *Angew. Chem., Int. Ed.* **2005**, *44*, 1826.

(22) If a smaller amount of catalyst is used (10 mol %), the reaction is very slow and a longer reaction time is needed to reach a high conversion.

(23) A different procedure for recycling the catalyst was then attempted: after the Diels–Alder reaction, catalyst 3 was recovered by centrifugation, suspended in DMF, and stirred at 80 °C for 6 h with the aim of dissolving the insoluble organic residues (mainly cyclopentadiene dimer), which could occlude the mesopores. After this treatment and after addition of HBF<sub>4</sub>, catalyst 3 was reused in the cycloaddition of cyclopentadiene and cinnamic aldehyde, affording the products in 30% yield.

(24) In order to overcome the recycling problems, silica-supported imidazolidinones have found application in continuous flow chemistry processes: Chirolì, V.; Benaglia, M.; Cozzi, F.; Puglisi, A.; Annunziata, R.; Celentano, G. *Org. Lett.* **2013**, *15*, 3590.

(25) Shi, J. Y.; Wang, C. A.; Li, Z. J.; Wang, Q.; Zhang, Y.; Wang, W. *Chem. Eur. J.* **2011**, *17*, 6206.

## ■ NOTE ADDED AFTER ASAP PUBLICATION

In the version reposted on November 15, 2013 there are text changes and updates to references 14 and 25.